ACS APPLIED MATERIALS & INTERFACES

Research Article

www.acsami.org

Cyclodextrin-Modified Porous Silicon Nanoparticles for Efficient Sustained Drug Delivery and Proliferation Inhibition of Breast Cancer Cells

Alexandra Correia,[†,§] Mohammad-Ali Shahbazi,[†,§] Ermei Mäkilä,[†,‡] Sérgio Almeida,[†] Jarno Salonen,[‡] Jouni Hirvonen,[†] and Hélder A. Santos*[,†]

[†]Division of Pharmaceutical Chemistry and Technology, Faculty of Pharmacy, University of Helsinki, FI-00014 Helsinki, Finland

[‡]Laboratory of Industrial Physics, Department of Physics and Astronomy, University of Turku, FI20014 Turku, Finland

Supporting Information

ABSTRACT: Over the past decade, the potential of polymeric structures has been investigated to overcome many limitations related to nanosized drug carriers by modulating their toxicity, cellular interactions, stability, and drug-release kinetics. In this study, we have developed a successful nanocomposite consisting of undecylenic acid modified thermally hydrocarbonized porous silicon nanoparticles (UnTHCPSi NPs) loaded with an anticancer drug, sorafenib, and surface-conjugated with heptakis(6-amino-6-deoxy)-β-cyclodextrin (HABCD) to show the impact of the surface polymeric functionalization on the physical and biological properties of the drug-loaded nanoparticles. Cytocompatibility studies showed that the UnTHCPSi−HABCD NPs were not toxic to breast cancer cells. HABCD also enhanced the suspensibility and both the colloidal and plasma stabilities of the UnTHCPSi NPs. UnTHCPSi−HABCD NPs showed a significantly increased interaction with breast cancer cells compared to bare NPs and also sustained the drug release. Furthermore, the sorafenib-loaded UnTHCPSi−HABCD NPs efficiently inhibited cell proliferation of the breast cancer cells.

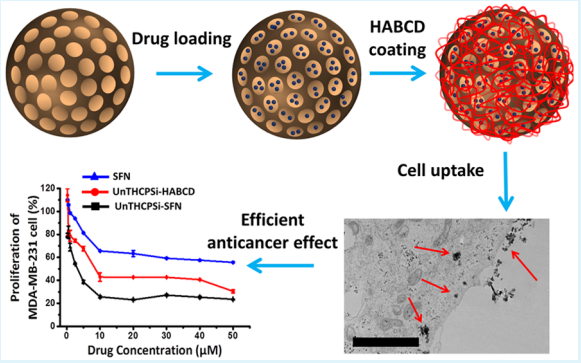

KEYWORDS: *cyclodextrin, porous silicon, anticancer nanocomposite, drug delivery, cellular interactions*

1. INTRODUCTION

The progress in nanotechnology has been perceptible over the past decades owing to its potential in disease prevention, diagnosis, and treatment.[1] While various biomaterials have been introduced for nanomedical applications, porous silicon nanoparticles (PSi NPs) have attracted intensive attention as versatile vehicles for various biomedical applications, including drug delivery and bioimaging, because of their facile fabrication process, adjustable pore size, easily obtained functionalization chemistries, high safety, high surface area, biocompatibility, biodegradability, and capability to be used as carriers for different payloads.[2−5]

For drug-delivery applications, therapeutic molecules can be loaded in the porous structure or immobilized on the external surface of the PSi NPs by a proper conjugation method. However, bare NPs loaded with drugs by encapsulation or conjugation may suffer from some limitations, such as burst drug release, lack of protection from enzymatic degradation, and low stability in aqueous media. To overcome these shortcomings, it has been recently suggested to apply polymers as substrates for preparing PSi-based composites that can render new physicochemical and biological advantages, such as improved control over drug release, improved stability in aqueous solution, and modification of the NP's behavior at the biointerfaces of the NPs.[6−8]

Recently, the idea of using cyclodextrins (CDs) as biodegradable polymers has gained increased interest.[9,10] CDs are cyclic oligosaccharide polymers[11] with unique properties for biomedical applications, such as long-term biocompatibility, low toxicity, and a lack of immune stimulation, indicating their potential for making building blocks of nanoparticulate carriers of interest.[12,13] Different kinds of CD derivatives have recently been developed for various pharmaceutical applications, including improved solubility of poorly water-soluble drugs, sustained drug release by making cross-linked nanonetworks or drug−polymer nanoconjugates, and improved drug stability and bioavailability in vivo.[14] There are many reports in the literature showing the encapsulation of drug molecules into the CD matrix or the surface modification of NPs with CD with the aim of facilitating the safe and efficient delivery of drugs.[15−17] For example, Zhao et al. have reported the pH- and enzyme-sensitive release of two drugs from CD-gated mesoporous silica nanovehicles.[18] Cheng et al. have also shown a highly efficient

Received: July 31, 2015
Accepted: October 5, 2015
Published: October 6, 2015

DOI: 10.1021/acsami.5b07033
ACS Appl. Mater. Interfaces 2015, 7, 23197−23204

anticancer effect of mesoporous silica nanoparticles coated with α-CD anchored onto the pore entrances of the mesoporous silica nanoparticles as gatekeeper molecules controlling the doxorubicin release from the pores in an enzyme-responsive manner.[19]

Heptakis(6-amino-6-deoxy)-β-cyclodextrin (HABCD) is a new derivative of CD with improved physicochemical properties and enhanced hydrophilicity by substituting the hydroxyl groups of native CDs,[20,21] with the aim of expanding the potential of CDs in pharmaceutical applications. These CDs are very attractive for drug-delivery applications because of their favorable safety profile and ability to work as capping molecules to cover the pores of porous carriers and to protect the loaded compounds from the external environment. Owing to these advantages, CDs have attracted interest for the delivery a specific amount of therapeutics in a defined period of time to a specific part of the body.[10,22]

The chemotherapeutic drug sorafenib (SFN) is currently suggested for cancer treatment; however, in order to reduce its systemic toxicity and side effects, it is important to investigate its possible delivery using nanocarriers. For example, Zhang et al.[23] have developed SFN-loaded albumin NPs with reduced hemolysis and myelosuppression effect compared to the free drug. SFN-loaded poly[(lactic/glycolic) acid] was also suggested by Liu et al.[24] to efficiently improve the toxicity of the drug on tumor cells. Nevertheless, controlling the SFN release from NPs has remained a big challenge because of its poor water solubility. To solve the problem, polymeric coating of the porous NPs loaded with SFN can be a promising strategy for the delivery of this drug because the porous structure of PSi can increase the solubility of the drug and the polymer can act as a gate keeper for controlling the drug release. Thus, by applying a polymer on the surface of the PSi NPs, which is also able to minimize plasma protein absorption on the surface of the particles, one can develop a long-circulating drug-delivery nanocomposite. Therefore, we hypothesize that HABCD-coated PSi NPs can be a promising approach for the delivery of SFN. Moreover, compared to the free drugs used for breast cancer therapy, nanomedicines may result in better drug distribution in the body and enhance the therapeutic efficacy.[25,26]

In this work, we have used undecylenic acid functionalized thermally hydrocarbonized porous silicon (UnTHCPSi) NPs conjugated with HABCD to study the impact of surface polymeric functionalization on the physical and biological properties of the drug-loaded NPs. Studies of the cytocompatibility, stability of the NPs in aqueous buffer as well as human plasma, cellular association, drug-release profile modification after polymeric coating, and anticancer effect on MCF-7 and MDA-MB-231 breast cancer cells were evaluated.

2. EXPERIMENTAL SECTION

2.1. Synthesis of the UnTHCPSi NPs. The procedure for the preparation of PSi NPs was performed as described elsewhere.[27,28] All of the experimental details are reported in the Supporting Information.

2.2. Preparation of UnTHCPSi–HABCD NPs. To prepare UnTHCPSi–HABCD NPs, the amine groups of HABCD were covalently conjugated to the carboxyl groups of UnTHCPSi NPs by 1-ethyl-3-[3-(dimethylamino)propyl]carbodiimide hydrochloride (EDC)/*N*-hydroxysuccinimide (NHS) chemistry. For this purpose, a solution of EDC (17 mM) was prepared in 10 mM 2-(*N*-morpholino)ethanesulfonic acid saline buffer at pH 5.5, and NHS (10.2 mM) was prepared in phosphate-buffered saline (PBS) at pH 7.2. For covalent conjugation, UnTHCPSi NPs (1 mg) were dispersed in 330 μL of EDC and NHS in the darkness, followed by dispersion and mixing for 120 min to activate the carboxyl groups present on the surface of the PSi NPs. Then, chemically activated PSi NPs were treated with an excess amount of HABCD with a 1:10 ratio (NPs–HABCD) with stirring (300 rpm) in the dark and at room temperature overnight. The excess of unconjugated HABCD was removed by extensive washing twice with Milli-Q water.

2.3. Physicochemical Characterization of the Nanocomposites. A Zetasizer Nano ZS instrument (Malvern Instruments Ltd., U.K.) was used to measure the hydrodynamic size (*Z*-average), polydispersity index (PDI), and surface ζ potential of the developed NPs (see further experimental details in the Supporting Information).

2.4. Stability in Human Plasma and Aqueous Solution. For the stability tests, all of the experimental details are reported in the Supporting Information.

2.5. Cell Lines and Culture Conditions. The cancer cells tested were MCF-7 and MDA-MB-231 breast carcinoma cells obtained from American Type Culture Collection and cultured in 75 cm^2 culture flasks (Corning Inc. Life Sciences, USA). These cells were cultured in a standard BB 16 gas incubator (Heraeus Instruments GmbH, Germany) set at 95% humidity, 5% CO_2, and 37 °C. MCF-7 and MDA-MB-231 breast cancer cells were cultured in Dulbecco's modified Eagle's medium and in standard Roswell Park Memorial Institute 1640 media, respectively, both supplemented with 10% (v/v) fetal bovine serum (FBS), 1% nonessential amino acids, 1% L-glutamine, penicillin (100 IU/mL), and streptomycin (100 mg/mL) (all from HyClone, USA). Cells' subculturing was conducted at 80% confluency, harvested prior to cell passaging and each experiment with trypsin–PBS–ethylenediaminetetraacetic acid.

2.6. Cellular Toxicity Studies. To evaluate the biosafety of the NPs, the viability of rat isolated liver and kidney cells was assessed by measuring their ATP activity after exposure to the NPs. For this purpose, Wistar rats weighing between 250 and 275 g were sacrificed by decapitation, and the kidney and liver organs were excised, cut into small pieces, and collected in a clean 6-well plate dish containing 3 mL of PBS. The cells were then minced through a 70 μm cell strainer, and the dispersed cell solution was collected in 10 mL of PBS (pH 7.4). The cells were then washed twice by centrifugation at 900 rpm for 5 min at 4 °C and were then resuspend in Hank's balanced salt solution (HBSS)–4-(2-hydroxyethyl)-1-piperazineethanesulfonic acid (HEPES) containing 10% FBS. The cells were then counted, and the concentration was adjusted to 40000 cells/100 μL of HBSS–HEPES containing 10% FBS. After that, 50 μL of the cell suspension was added into each well of the 96-well plates, and 50 μL portions of the NPs with concentrations of 50, 100, and 200 μg/mL were added to make final concentrations of 25, 50, and 100 μg/mL. After 24 h of incubation at 37 °C, the reagent assay (100 μL; CellTiter-Glo Luminescent Cell Viability Assay, Promega, USA) was added to each well. The luminescence was measured using a Varioskan Flash (Thermo Fisher Scientific Inc., USA). Positive (1% Triton X-100) and negative HBSS buffer (pH 7.4) + 10% FBS controls were also used and the cells treated similarly as described above. At least three independent measurements were conducted for each experiment. The cellular toxicity was also conducted on the breast cancer cells, and the experimental procedure is explained in detail in the Supporting Information.

The anticancer effect of the developed nanocomposites on cancer cells was also monitored by measuring the antiproliferation effect of the free SFN and drug-loaded NPs using the same method as explained above.

2.7. Cellular Interaction Studies. To investigate the ability of NPs to interact with cells, transmission electron microscopy (TEM) was performed after the NPs were exposed to MCF-7 and MDA-MB-231 cells (for further experimental details, see the Supporting Information).

2.8. Flow Cytometry Analyses of Cellular Interaction. MCF-7 and MDA-MB-231 cells were incubated at 37 °C in 6-well plates overnight to perform the studies of flow cytometry analyses. The full details of this experiment are reported in the Supporting Information.

DOI: 10.1021/acsami.5b07033
ACS Appl. Mater. Interfaces 2015, 7, 23197–23204

2.9. Loading Degree and Release Study. The anticancer drug SFN was loaded within the pores of the NPs by an immersion method and by dispersion of the particles in a concentrated solution of the drug. The experimental details are described in detail in the Supporting Information.

Ethics. All experimental protocols with animals were approved by the Laboratory Animal Center of the University of Helsinki and National Animal Experiment Board of Finland and conform to the EU's Guidelines for Accommodation and Care of Animals, following the Act (497/2013) and the Decree (564/2013) on Animal Experimentation approved by the Finnish Ministry of Agriculture and Forestry and the EU Directive (2010/63/EU).

2.10. Statistical Analyses. In all experiments, the obtained values are reported as mean ± standard deviation (s.d.) from three independent measurements. One-way analysis of variance (ANOVA) was used to statistically evaluate the obtained values with the level of significance set at probabilities of (*) $p < 0.05$, (**) $p < 0.01$, or (***) $p < 0.001$. *GraphPad Prism 5* software (GraphPad Software Inc., USA) was used for the statistical analyses.

3. RESULTS AND DISCUSSION

3.1. Fabrication and Characterization of the UnTHCPSi NPs and HABCD-Conjugated UnTHCPSi. Fabrications of NPs with high stability and safety, desirable drug-release profiles, and efficient cellular uptake are the main challenges for the development of NPs with high potential to be applied in nanomedicine. As a result of the promising results showed in the recent literature about the potential of the UnTHCPSi NPs for drug-delivery applications,[8,29] the surface of these particles is functionalized with HABCD in this study to further adjust desirable physicochemical and biological properties of the NPs for cancer therapy purposes. An EDC/NHS chemistry method was used to conjugate HABCD onto the surface of bare particles in an aqueous solution. To functionalize the surface of the particles with a HABCD polymer, the carboxyl groups of the NPs were activated and covalently conjugated to the amine groups of HABCD to form UnTHCPSi–HABCD nanocomposites.

The average particle size of bare UnTHCPSi NPs, measured by dynamic light scattering (DLS), increased from 227.0 ± 0.2 to 388.5 ± 1.2 nm after HABCD conjugation on the surface of the particles. As expected, the negative ζ-potential of UnTHCPSi NPs (−29.1 ± 0.5 mV) was changed to positive after HABCD conjugation (+24.3 ± 0.8 mV) owing to the amine group in the structure of HABCD,[30] indicating successful HABCD conjugation on the surface of NPs. The PDI of UnTHCPSi and UnTHCPSi–HABCD NPs before and after conjugation was ca. 0.12, demonstrating the monodispersity of the NPs. The surface area, pore volume, and pore size of the PSi NPs were 282 ± 7 m^2/g, 0.75 ± 0.06 cm^3/g, and 10.7 ± 0.7 nm, respectively, measured by the previously reported methods.[3,5]

To further assess the successful chemical covalent conjugation of HABCD to the carboxylic groups of the particles, attenuated total reflectance Fourier transform infrared (ATR-FTIR) measurements were performed. As shown in Figure 1, the spectrum of the UnTHCPSi NPs with bands at 2950, 1710, and 1459 cm^{-1} corresponds to the C–H stretching, carbonyl C=O stretching, and CH_2 deformation, respectively.[8] The ATR-FTIR spectrum of HABCD showed a small band in the range of 1580–1650 cm^{-1} assigned to the presence of a N–H bend (amide II).[31] The band at around 1590 cm^{-1} of the UnTHCPSi–HABCD NPs is also indicative of amide II (presented in the HABCD structure), which confirmed the conjugation of HABCD on the UnTHCPSi NPs' surface.

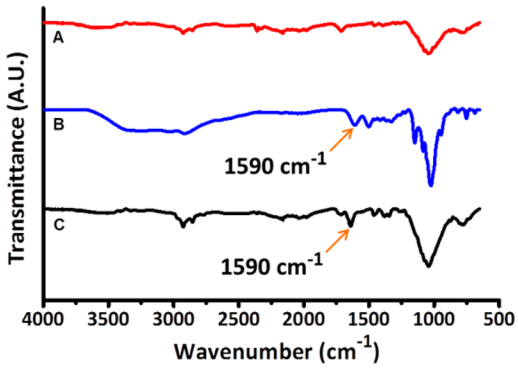

Figure 1. ATR-FTIR spectra of UnTHCPSi NPs (A), HABCD (B), and UnTHCPSi–HABCD NPs (C). The obtained spectrum for the HABCD-conjugated NPs confirms the chemical conjugation and the formation of the desired nanocomposite.

3.2. Stability of the HABCD-Conjugated NPs. It is important to evaluate the interactions of the NPs with human plasma, in order to understand and evaluate the stability of the developed nanocomposites after in vivo intravenous administration. NPs are rapidly contacting with plasma proteins when they enter the blood circulation. In order to prevent NP agglomeration and rapid clearance by the immune cells, the NPs should present minimal interactions with the plasma proteins. Therefore, it is important to determine the change in the properties of the NPs, especially in terms of size, because the plasma proteins can selectively bind to the surface of the NPs[28] and change their biological behavior.[29]

To improve the NPs' plasma stability, different kinds of biopolymers like HABCD can be conjugated to their surface for better resistance to the protein adsorption.[32,33] The plasma stability results revealed that the HABCD-crosslinked NPs could reduce variation in the size and PDI compared to bare UnTHPSi NPs dispersed in plasma, mainly because of fewer plasma protein interactions with the particles (Figure 2A,B), and thus, improving the stability of the PSi NPs conjugated with HABCD. For bare UnTHCPSi NPs, the size was increased from an average of ca. 201–337 nm after 30 min in contact with human plasma, whereas the size of UnTHCPSi–HABCD increased from ca. 211 to 241 nm after 30 min (Figure2A). This clearly indicates that there is a less interaction with human plasma for the HABCD-conjugated PSi NPs. The PDI in a plasma solution increased less for HABCD-conjugated NPs than for bare NPs.

In the case of the colloidal stability in PBS, it was observed that the hydrodynamic size and PDI of bare UnTHCPSi NPs increased from ca. 222 to 843 nm and from 0.1 to 0.203, respectively, in 30 min as a result of NP aggregation. Contrarily, the HABCD-conjugated PSi NPs showed no significant changes in the particle size and PDI. This was due to the conjugation of HABCD on the surface of the NPs, which helped to prevent strong aggregation of the NPs because of the increased hydrophilicity of the surfaces of the UnTHCPSi NPs (Figure 2C,D).[34] The improved stability results of the PSi NPs and decreased aggregation in plasma demonstrates the potential benefits for the future systemic administration of these nanocomposites.

To confirm the results of the colloidal stability and changes in the surface properties of the particles after the HABCD conjugation, TEM imaging was used to characterize all of the NPs (Figure 3) in PBS. Aggregation of the UnTHCPSi NPs in

DOI: 10.1021/acsami.5b07033
ACS Appl. Mater. Interfaces 2015, 7, 23197–23204

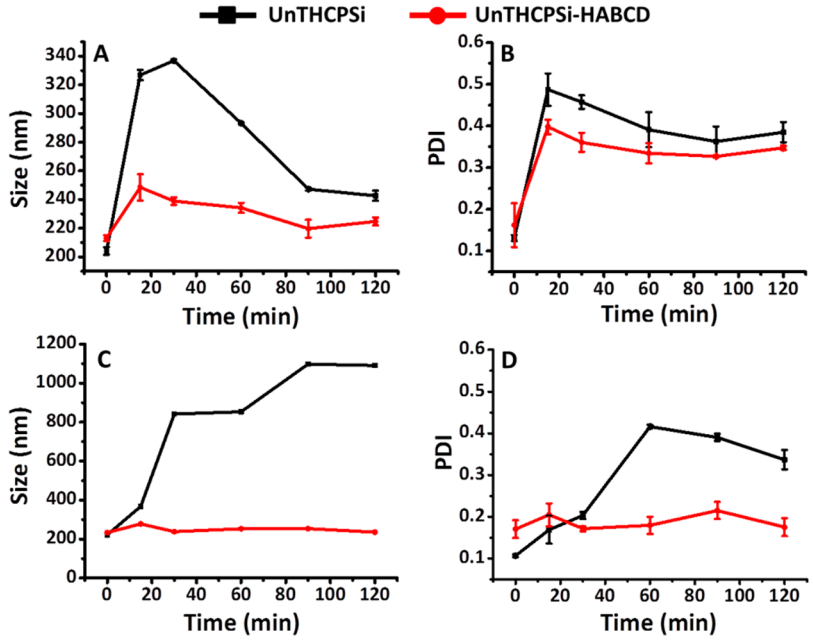

Figure 2. Change in the size (A and C) and PDI (B and D) of the NPs after 2 h of incubation in human plasma (A and B) and aqueous solution (C and D). The size variation was minimal for HABCD-conjugated NPs in both human plasma proteins (A) and aqueous solution (C), while UnTHCPSi NPs showed a big change in the size and PDI in both media. The experiments were performed in triplicate, and all represented values show the mean ± s.d. (n = 3).

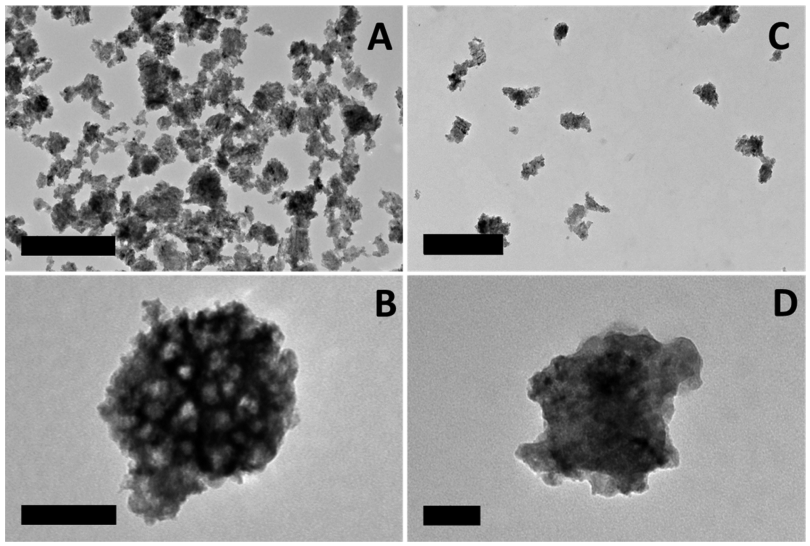

Figure 3. TEM images of the UnTHCPSi NPs (A and B) and UnTHCPSi–HABCD NPs (C and D) NPs with low and high magnification at the same NP concentration (50 μg/mL). Scale bars are 500 nm for the lower magnification (A and C) and 100 nm for the higher magnification (B and D).

PBS was observed because of the hydrophobicity of the particles. In fact, the UnTHCPSi NPs did not form stable dispersion in PBS and, thus, could be more prone to aggregation (Figure 3A,B). After conjugation with HABCD, the PSi NPs showed high dispersion and less aggregation in PBS (Figure 3C,D). The morphological change observations also showed that the UnTHCPSi NPs possess irregular shape with visible pores in their structure (Figure 3B), while HABCD covers the surface of the UnTHCPSi NPs (Figure 3D), and no pores are visible in this case. This indicates that the polymer is able to form a layer on the surface of the UnTHCPSi NPs through chemical conjugation to the carboxylic groups on the surface of the UnTHCPSi NPs. This confirms that the polymer can act as a gate keeper to retain drug molecules inside the pores of the UnTHCPSi NPs.

3.3. Cellular Viability Studies. To show high safety and in vitro cytocompatibility of the UnTHCPSi and UnTHCPSi–HABCD NPs, the ATP activity of kidney and liver cells of a healthy rat was measured after 24 h of incubation with different concentrations of the NPs. The ATP activity of the MDA-MB-231 and MCF-7 cancer cells was also measured,[29,35,36] and all of the results are shown and discussed in detail in Figure S1 in the Supporting Information.

As shown in Figure 4, for both kidney and liver cells, the NPs showed very high safety in all measured concentrations; however, the lower tested concentrations of both the

DOI: 10.1021/acsami.5b07033
ACS Appl. Mater. Interfaces 2015, 7, 23197–23204

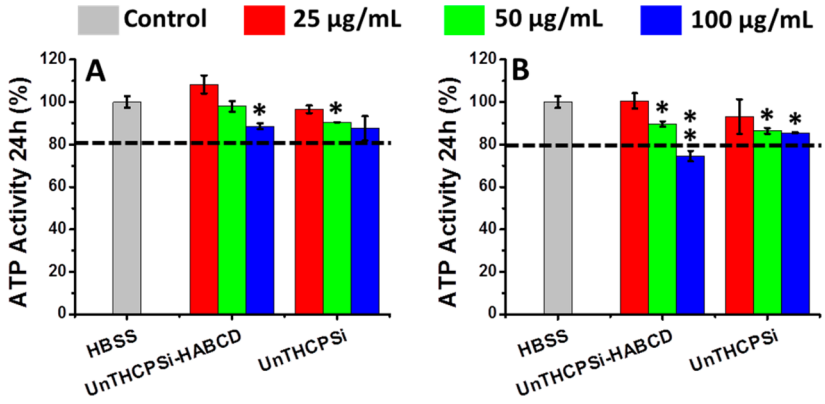

Figure 4. Cell viability study on kidney (A) and liver (B) cells obtained from healthy rats after incubation with the UnTHCPSi–HABCD and UnTHCPSi NPs for 24 h. Statistical analyses were performed by ANOVA. A HBSS solution (pH 7.4) + 10% FBS was used as the negative control. The levels of significances were set at probabilities of (*) $p < 0.05$, (**) $p < 0.01$, and (***) $p < 0.001$. Error bars show the s.d. ($n \geq 3$).

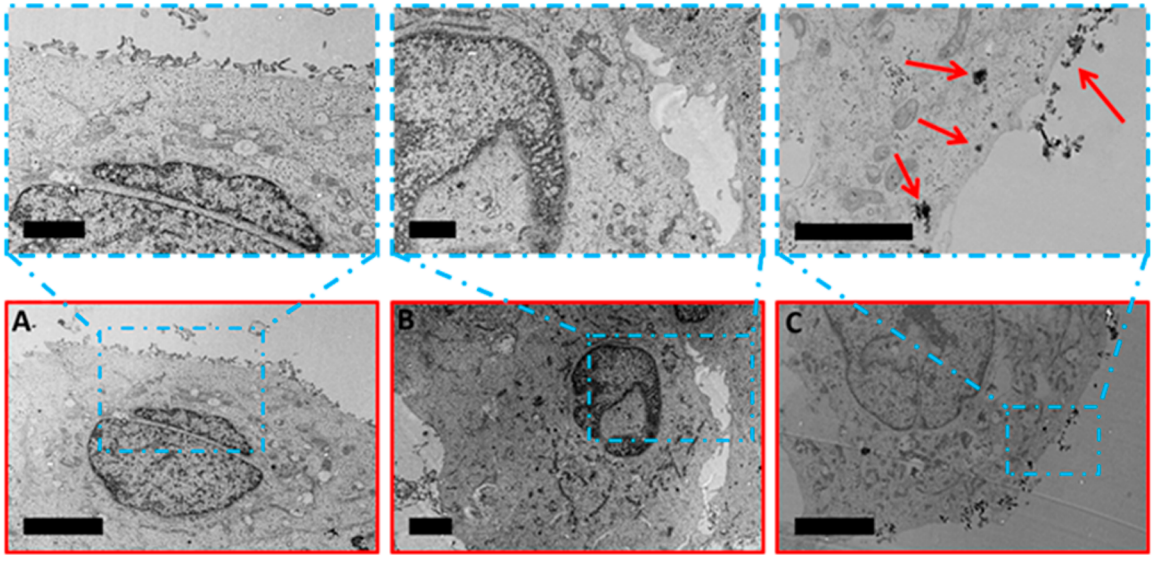

Figure 5. TEM images of MCF-7 (A), MCF-7 with the UnTHCPSi NPs (B), and MCF-7 with the UnTHCPSi–HABCD NPs (C) after 6 h of incubation. Red arrows show polymer-coated NPs interacting with the cell membrane or localized inside the MCF-7 cells. Scale bars are 2 and 5 μm for the lower and upper rows, respectively.

UnTHCPSi–HABCD and UnTHCPSi NPs were, in general, safer than those at high NP concentrations. These results indicate the high safety of the HABCD-conjugated NPs for drug delivery applications and breast cancer therapy. The very low cytotoxicity of the UnTHCPSi NPs in the tested concentrations is ascribed to the low cellular interactions of the particles due to the low aqueous stability and subsequent aggregation, as well as negative surface charge of the NPs.[7] Considering the positive charge of the HABCD-conjugated PSi NPs, these results confirmed that HABCD conjugation on PSi NPs can probably increase the NP–cell interactions because of the charge conversion from negative to positive, while preserving the safety of the negative-charge UnTHCPSi NPs that have, in general, low cellular association, as shown in section 3.4.

3.4. Cellular Association Evaluation. Major concerns of nanomedicines for cancer therapy are the efficient drug delivery and facile interactions of the NPs with the cancer cells, which have to take place during a limited period of time. Although the size of the NPs has a critical impact on the cellular association of the NPs, the chemical composition has also shown a significant impact on the interaction at the cellular level by changing some of the properties of the NPs, including the dispersibility, biocompatibility, and hydrophilicity.[35,36] The TEM images in Figure 5A–C show that bare UnTHCPSi NPs have very poor interaction with the MCF-7 cancer cells, while the HABCD-conjugated PSi NPs present high cellular association. This observation can be attributed to the improved dispersity of the NPs and their positive surface charge.

Flow cytometry analyses were also performed to confirm the TEM observations (Figure 6), showing a significant increase in the percentage of cells interacting with the UnTHCPSi NPs after conjugation with HABCD. These results showed that the percentages of cells interacting with the UnTHCPSi NPs are 28.6 ± 10.7% and 26.4 ± 7.3% after 6 and 24 h, respectively. In contrast, polymeric coating of the NPs resulted in a high increase in the cell–NP interactions to 71.7 ± 8.7% and 92.1 ± 3.6% after 6 and 24 h, respectively. These data corroborate the potential of such nanocomposites for further intracellular drug delivery applications.

3.5. Drug Loading and Release. In order to investigate the drug-loading capability of the NPs, the amount of the

DOI: 10.1021/acsami.5b07033
ACS Appl. Mater. Interfaces 2015, 7, 23197–23204

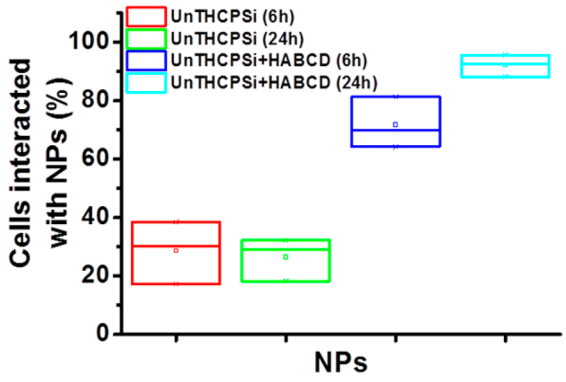

Figure 6. Flow cytometry analysis of the percentage of MCF-7 cells associated with the UnTHCPSi and UnTHCPSi−HABCD NPs after 6 and 24 h of incubation.

loaded drug was compared before and after HABCD conjugation. SFN, a very poorly water-soluble anticancer drug,[37] was used as a model drug to investigate the loading in bare UnTHCPSi and UnTHCPSi−HABCD NPs, as well as to evaluate the release in a HBSS solution at pH 7.4 and 5.5. The loading degree of SFN in bare UnTHCPSi NPs was 13.6 ± 2.1%, while the loading degree of UnTHCPSi−HABCD NPs was 17.7 ± 0.8%. The increase of the loading degree in the UnTHCPSi−HABCD NPs was probably due to the localization of the drug molecules inside the UnTHCPSi NP pores and also within the HABDC matrix on the surface of the particles.[9]

The profiles of SFN release from drug-loaded PSi NPs were also studied before and after HABCD conjugation (Figure 7). For pure SFN, very slow drug dissolution was observed as expected because of its poor solubility in aqueous solutions.[29] One of the main aims for nanobased cancer therapy is to develop nanosystems for sustained drug release[38] and, consequently, to improve the therapeutic efficiency and minimize the toxicity of the anticancer drug molecules. One of the most important benefits of the bare PSi NPs is the substantial enhancement of the solubility of poorly water-soluble drug compounds via inhibition of crystallization of the drugs inside the pores; the amorphous-like form of drug molecules can rapidly dissolve in the aqueous medium and release very fast.[39] In order to develop nanosystems that can more effectively control and sustain the release of drugs from PSi, HABCD was conjugated on the surface of bare UnTHCPSi NPs. The results showed that the dissolution of pure SFN was less than 5% at both pH values tested, while the UnTHCPSi NPs released 60% and 80% of the drug after 4 h at pH 7.4 and 5.5, respectively. In contrast, the release of SFN from the UnTHCPSi−HABCD NPs in a HBSS solution was around 40% at both pH values tested. These results suggest that HABCD can more effectively retain SFN inside and sustain the drug release from the PSi NPs.

3.6. Antiproliferation Effect on Breast Cancer Cells. To confirm that the UnTHCPSi−HABCD NPs can efficiently modulate the anticancer effect of SFN by sustaining the release of the drug, the cell proliferation profile of the breast cancer cells was screened after treatment with the free SFN and SFN-loaded NPs. The results displayed that free SFN has a poor proliferation inhibition profile by reducing the percentage of viable cells to 90% and 60% for MCF-7 (Figure 8A) and MDA-MB-231 cells, respectively, at the highest concentration (Figure 8A,B). For UnTHCPSi and UnTHCPSi−HABCD NPs, a higher reduction in the ATP activity was observed as expected because of the improved drug solubility when the drug was loaded into the pores of the NPs and a sustained release due to the polymeric coating. As for the drug-loaded UnTHCPSi NPs, the viability decreased from around 90% to 60% and from around 90% to 30%, for MCF-7 and MDA-MB-231 breast cancer cells, respectively. The drug-loaded HABCD-conjugated PSi NPs also exhibited a decrease in the proliferation profiles from around 110% to 80% and from around 110% to 40% for MCF-7 and MDA-MB-231, respectively. This was attributed to the conjugation of HABCD on the PSi NPs' surface, keeping the free drug inside the pores, thus slowing down the drug release and reducing the contact of SFN with the cells compared to the SFN−UnTHCPSi NPs.

Overall, these results are in agreement with the drug release studies that showed that the HABCD-conjugated PSi NPs can more efficiently sustain the drug release. Thus, the developed nanocarrier is envisaged as a potential candidate for cancer therapy. Very slow drug release in the blood circulation and increased cellular uptake by employing the HABCD-conjugated PSi NPs can be considered a good combination for drug delivery to cancer cells.[17,40,41] This may improve the efficiency of cancer treatment and also minimize the side effects of anticancer drugs.

4. CONCLUSIONS

Parallel to rapid and intense advances in nanomedicine, surface modification of the NPs by different macromolecules is necessary with the aim to achieve cell reactivity balance, reduced toxicity, stability enhancement, controllable cellular interactions, and an enhanced therapeutic effect. For this

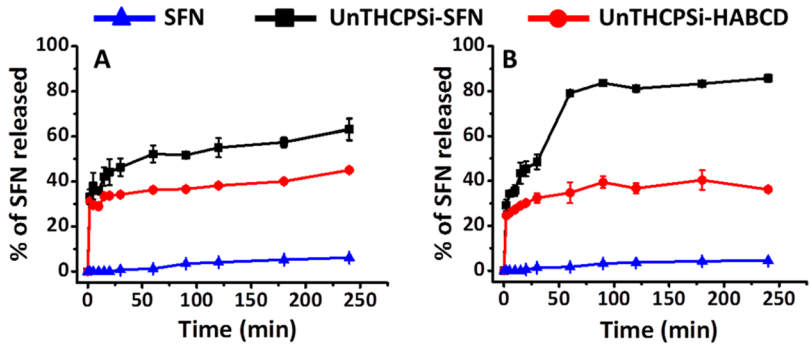

Figure 7. SFN release pattern from the UnTHCPSi and UnTHCPSi−HABCD NPs in the HBSS solution at pH 7.4 (A) and pH 5.5 (B) at 37 °C in the presence of 10% FBS. Values show the mean ± s.d. (n = 3).

DOI: 10.1021/acsami.5b07033
ACS Appl. Mater. Interfaces 2015, 7, 23197−23204

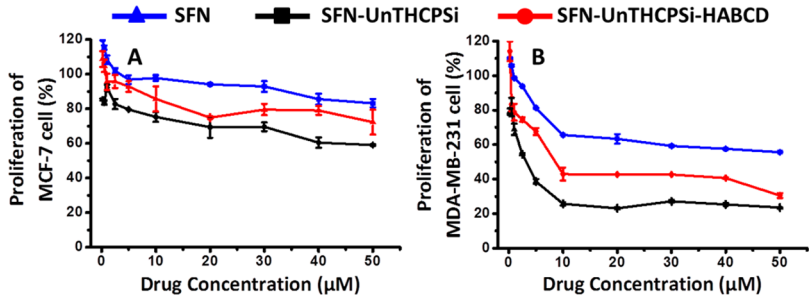

Figure 8. Proliferation of MCF-7 (A) and of MDA-MB-231 (B) cells after exposure to free SFN, SFN−UnTHCPSi NPs, and SFN−UnTHCPSi−HABCD NPs for 24 h at 37 °C. A HBSS solution (pH 7.4) containing 10% FBS was used to suspend the NPs. Samples were prepared by dilution of the highest drug concentration using HBSS containing 10% FBS. The data show the mean ± s.d. (n = 3). A HBSS solution (pH 7.4) was used as the negative control with 100% proliferation.

purpose, we have successfully conjugated the HABCD polymer on the PSi NPs surface, aiming to reduce the NPs' toxicity, increase their stability, enhance the cell−NP interactions, and sustain the loaded drug release. In this study, we observed that while HABCD had no toxic effect on the MCF-7 and MDA-MB-231 breast cancer cells and did not change the cytotoxicity profiles of bare UnTHCPSi, the polymeric conjugation significantly sustained drug release in aqueous solutions. For the colloidal stability in PBS, we observed that the modulated surface properties and increased hydrophilicity of the HABCD-functionalized NPs could extensively minimize NP aggregation via enhanced charge repulsion and suspensibility compared to UnTHCPSi NPs. Furthermore, UnTHCPSi−HABCD NPs showed increased in vitro interactions with both MDA-MB-231 and MCF-7 breast cancer cells at the biointerface. Moreover, the cell proliferation inhibition efficacy of SFN-loaded UnTHCPSi−HABCD NPs was enhanced compared to that of SFN−UnTHCPSi NPs at the studied time points. The results showed that HABCD-coated NPs reduced the PDI, favorably modulated the colloidal and human plasma stabilities, and increased the NP's accumulation inside the cells, indicating the potential of such systems for intracellular drug delivery. It was also shown that HABCD-conjugated NPs were able to keep SFN molecules within the pores, leading to a sustained drug release. This study and all results shown represent a proof-of-concept that the coating of the PSi NPs with HABCD renders new advantageous properties to the particles for drug delivery applications.

■ ASSOCIATED CONTENT

Supporting Information

The Supporting Information is available free of charge on the ACS Publications website at DOI: 10.1021/acsami.5b07033.

Experimental details on the synthesis and physicochemical characterization of the nanocomposites, stability study, cellular toxicity and interactions, flow cytometry, loading degree and release study protocols, and results of the viability studies in cancer cells (PDF).

■ AUTHOR INFORMATION

Corresponding Author

*E-mail: helder.santos@helsinki.fi (H.A.S.).

Author Contributions

§Authors contributed equally to this work.

Notes

The authors declare no competing financial interest.

■ ACKNOWLEDGMENTS

Dr. H. A. Santos acknowledges financial support from the Academy of Finland (Nos. 252215 and 281300), the University of Helsinki Research Funds, the Biocentrum Helsinki, and the European Research Council under the European Union's Seventh Framework Programme (FP/2007-2013; Grant 310892).

■ REFERENCES

(1) Liu, Y.; Miyoshi, H.; Nakamura, M. Nanomedicine for Drug Delivery and Imaging: A Promising Avenue for Cancer Therapy and Diagnosis Using Targeted Functional Nanoparticles. *Int. J. Cancer* **2007**, *120*, 2527−2537.

(2) Herranz-Blanco, B.; Liu, D.; Mäkilä, E.; Shahbazi, M.; Ginestar, E.; Zhang, H.; Aseyev, V.; Balasubramanian, V.; Salonen, J.; Hirvonen, J.; Santos, H. A. On-Chip Self-Assembly of a Smart Hybrid Nanocomposite for Antitumoral Applications. *Adv. Funct. Mater.* **2015**, *25*, 1488−1497.

(3) Shahbazi, M. A.; Fernandez, T. D.; Mäkilä, E. M.; Le Guevel, X.; Mayorga, C.; Kaasalainen, M. H.; Salonen, J. J.; Hirvonen, J. T.; Santos, H. A. Surface Chemistry Dependent Immunostimulative Potential of Porous Silicon Nanoplatforms. *Biomaterials* **2014**, *35*, 9224−9235.

(4) Wang, C.-F.; Mäkilä, E. M.; Kaasalainen, M. H.; Hagström, M. V.; Salonen, J. J.; Hirvonen, J. T.; Santos, H. A. Dual-Drug Delivery by Porous Silicon Nanoparticles for Improved Cellular Uptake, Sustained Release, and Combination Therapy. *Acta Biomater.* **2015**, *16*, 206−214.

(5) Shahbazi, M.-A.; Almeida, P.; Mäkilä, E. M.; Correia, A.; Ferreira, M.; Kaasalainen, M. H.; Salonen, J. J.; Hirvonen, J. T.; Santos, H. A. Poly(methyl vinyl ether-alt-maleic acid) Functionalized Porous Silicon Nanoparticles for Enhanced Stability and Cellular Internalization. *Macromol. Rapid Commun.* **2014**, *35*, 624−629.

(6) Zhang, H.; Liu, D.; Shahbazi, M.-A.; Mäkilä, E.; Herranz-Blanco, B.; Salonen, J.; Hirvonen, J.; Santos, H. A. Fabrication of a Multifunctional Nano-in-Micro Drug Delivery Platform by Microfluidic Templated Encapsulation of Porous Silicon in Polymer Matrix. *Adv. Mater.* **2014**, *26*, 4497−4503.

(7) Shrestha, N.; Shahbazi, M.-A.; Araújo, F.; Zhang, H.; Mäkilä, E.; Kauppila, J. M.; Sarmento, B.; Salonen, J.; Hirvonen, J.; Santos, H. A. Chitosan-Modified Porous Silicon Microparticles for Enhanced Permeability of Insulin Across Intestinal Cell Monolayers. *Biomaterials* **2014**, *35*, 7172−7179.

(8) Almeida, P.; Shahbazi, M.-A.; Mäkilä, E.; Kaasalainen, M.; Salonen, J.; Hirvonen, J.; Santos, H. A. Amine-modified Hyaluronic Acid-functionalized Porous Silicon Nanoparticles for Targeting Breast Cancer Tumors. *Nanoscale* **2014**, *6*, 10377−10387.

(9) Nguyen, M. K.; Alsberg, E. Bioactive Factor Delivery Strategies from Engineered Polymer Hydrogels for Therapeutic Medicine. *Prog. Polym. Sci.* **2014**, *39*, 1235−1265.

DOI: 10.1021/acsami.5b07033
ACS Appl. Mater. Interfaces 2015, 7, 23197−23204

(10) Tiwari, G.; Tiwari, R.; Rai, A. K. Cyclodextrins in Delivery Systems: Applications. *J. Pharm. BioAllied Sci.* **2010**, *2*, 72−79.
(11) Kurkov, S. V.; Loftsson, T. Cyclodextrins. *Int. J. Pharm.* **2013**, *453*, 167−180.
(12) Nafee, N.; Hirosue, M.; Loretz, B.; Wenz, G.; Lehr, C. M. Cyclodextrin-Based Star Polymers as a Versatile Platform for Nanochemotherapeutics: Enhanced Entrapment and Uptake of Idarubicin. *Colloids Surf., B* **2015**, *129*, 30−38.
(13) Draz, M. S.; Fang, B. A.; Zhang, P.; Hu, Z.; Gu, S.; Weng, K. C.; Gray, J. W.; Chen, F. F. Nanoparticle-Mediated Systemic Delivery of siRNA for Treatment of Cancers and Viral Infections. *Theranostics* **2014**, *4*, 872−892.
(14) Otero-Espinar, F. J.; Torres-Labandeira, J. J.; Alvarez-Lorenzo, C.; Blanco-Mendez, J. Cyclodextrins in Drug Delivery Systems. *Curr. Top. Med. Chem.* **2014**, *14*, 463−464.
(15) Abian, O.; Claveria-Gimeno, R.; Vega, S.; Grazu, V.; de la Fuente, J. M.; Lanas, A.; Velazquez-Campoy, A. Rescuing Compound Bioactivity in a Secondary Cell-Based Screening by Using Gamma-Cyclodextrin as a Molecular Carrier. *Int. J. Nanomed.* **2015**, *10*, 2249−2259.
(16) Zafar, N.; Fessi, H.; Elaissari, A. Cyclodextrin Containing Biodegradable Particles: From Preparation to Drug Delivery Applications. *Int. J. Pharm.* **2014**, *461*, 351−366.
(17) Calixto, G.; Bernegossi, J.; Fonseca-Santos, B.; Chorilli, M. *Int. J.* Nanotechnology-Based Drug Delivery Systems for Treatment of Oral Cancer: A Review. *Int. J. Nanomed.* **2014**, *9*, 3719−3735.
(18) Bai, L.; Zhao, Q.; Wang, J.; Gao, Y.; Sha, Z.; Di, D.; Han, N.; Wang, Y.; Zhang, J.; Wang, S. pH-Responsive Mesoporous Silica Nanoparticles Employed in Controlled Drug Delivery Systems for Cancer Treatment. *Nanotechnology* **2015**, *26*, 165704.
(19) Cheng, J.; Khin, K. T.; Jensen, G. S.; Liu, A.; Davis, M. E. Synthesis of Linear, β-Cyclodextrin-Based Polymers and Their Camptothecin Conjugates. *Bioconjugate Chem.* **2003**, *14*, 1007−1017.
(20) McCormack, B.; Gregoriadis, G. J. Entrapment of Cyclodextrin-Drug Complexes Into Liposomes: Potential Advantages in Drug Delivery. *Drug Target* **1994**, *2*, 449−454.
(21) Blanchemain, N.; Karrout, Y.; Tabary, N.; Bria, M.; Neut, C.; Hildebrand, H. F.; Siepmann, J.; Martel, B. Comparative Study of Vascular Prostheses Coated With Polycyclodextrins for Controlled Ciprofloxacin Release. *Carbohydr. Polym.* **2012**, *90*, 1695−1703.
(22) Moya-Ortega, M. D.; Alvarez-Lorenzo, C.; Concheiro, A.; Loftsson, T. Cyclodextrin-Based Nanogels for Pharmaceutical and Biomedical Applications. *Int. J. Pharm.* **2012**, *428*, 152−163.
(23) Zhang, J. Y.; He, B.; Qu, W.; Cui, Z.; Wang, Y. B.; Zhang, H.; Wang, J. C.; Zhang, Q. Preparation of the Albumin Nanoparticle System Loaded with Both Paclitaxel and Sorafenib and Its Evaluation in Vitro and in Vivo. *J. Microencapsulation* **2011**, *28*, 528−536.
(24) Liu, J.; Boonkaew, B.; Arora, J.; Mandava, S. H.; Maddox, M. M.; Chava, S.; Callaghan, C.; He, J.; Dash, S.; John, V. T.; Lee, B. R. Comparison of Sorafenib-Loaded Poly (Lactic/Glycolic) Acid and Dppc Liposome Nanoparticles in the in Vitro Treatment of Renal Cell Carcinoma. *J. Pharm. Sci.* **2015**, *104*, 1187−1196.
(25) Vinchon-Petit, S.; Jarnet, D.; Paillard, A.; Benoit, J. P.; Garcion, E.; Menei, P. In Vivo Evaluation of Intracellular Drug-Nanocarriers Infused into Intracranial Tumours by Convection-Enhanced Delivery: Distribution and Radiosensitisation Efficacy. *J. Neuro-Oncol.* **2010**, *97*, 195−205.
(26) Bae, Y.; Nishiyama, N.; Fukushima, S.; Koyama, H.; Yasuhiro, M.; Kataoka, K. Preparation and Biological Characterization of Polymeric Micelle Drug Carriers with Intracellular pH-Triggered Drug Release Property: Tumor Permeability, Controlled Subcellular Drug Distribution, and Enhanced in Vivo Antitumor Efficacy. *Bioconjugate Chem.* **2005**, *16*, 122−130.
(27) Araújo, F.; Shrestha, N.; Shahbazi, M.; Fonte, P.; Mäkilä, E. M.; Salonen, J. J.; Hirvonen, J. T.; Granja, P. L.; Santos, H. A.; Sarmento, B. The Impact of Nanoparticles on the Mucosal Translocation and Transport of GLP-1 Across the Intestinal Epithelium. *Biomaterials* **2014**, *35*, 9199−9207.
(28) Bimbo, L. M.; Sarparanta, M.; Santos, H. A.; Airaksinen, A. J.; Mäkilä, E.; Laaksonen, T.; Peltonen, L.; Lehto, V.-P.; Hirvonen, J.; Salonen, J. Biocompatibility of Thermally Hydrocarbonized Porous Silicon Nanoparticles and Their Biodistribution in Rats. *ACS Nano* **2010**, *4*, 3023−3032.
(29) Wang, C.-F.; Mäkilä, E. M.; Kaasalainen, M. H.; Liu, D.; Sarparanta, M. P.; Airaksinen, A. J.; Salonen, J. J.; Hirvonen, J. T.; Santos, H. A. Copper-Free Azide−Alkyne Cycloaddition of Targeting Peptides to Porous Silicon Nanoparticles for Intracellular Drug Uptake. *Biomaterials* **2014**, *35*, 1257−1266.
(30) Schofield, W. C.; McGettrick, J. D.; Badyal, J. P. A Substrate-Independent Approach for Cyclodextrin Functionalized Surfaces. *J. Phys. Chem. B* **2006**, *110*, 17161−17166.
(31) Casper, P.; Glöckner, P.; Ritter, H. Cyclodextrins in Polymer Synthesis: Free Radical Copolymerization of Methylated β-Cyclodextrin Complexes of Hydrophobic Monomers with N-Isopropylacrylamide in Aqueous Medium. *Macromolecules* **2000**, *33*, 4361−4364.
(32) Aggarwal, P.; Hall, J. B.; McLeland, C. B.; Dobrovolskaia, M. A.; McNeil, S. E. Nanoparticle Interaction With Plasma Proteins as it Relates to Particle Biodistribution, Biocompatibility and Therapeutic Efficacy. *Adv. Drug Delivery Rev.* **2009**, *61*, 428−437.
(33) McInnes, S. J.; Voelcker, N. H. Silicon-Polymer Hybrid Materials for Drug Delivery. *Future Med. Chem.* **2009**, *1*, 1051−1074.
(34) Sridhar, R.; Ramakrishna, S. Electrosprayed Nanoparticles for Drug Delivery and Pharmaceutical Applications. *Biomatter* **2013**, *3*, e24281.
(35) Shahbazi, M.; Hamidi, M.; Mäkilä, E. M.; Zhang, H.; Almeida, P.; Kaasalainen, M.; Salonen, J. J.; Hirvonen, J. T.; Santos, H. A. The Mechanisms of Surface Chemistry Effects of Mesoporous Silicon Nanoparticles on Immunotoxicity and Biocompatibility. *Biomaterials* **2013**, *34*, 7776−7789.
(36) Santos, H. A.; Riikonen, J.; Salonen, J.; Heikkilä, T.; Mäkilä, E.; Laaksonen, T.; Peltonen, L.; Lehto, V.-P.; Hirvonen, J. In Vitro Cytotoxicity of Porous Silicon Microparticles: Effect of the Particle Concentration, Surface Chemistry and Size. *Acta Biomater.* **2010**, *6*, 2721−2731.
(37) Szente, L.; Puskás, I.; Csabai, K.; Fenyvesi, É. Supramolecular Proteoglycan Aggregate Mimics: Cyclodextrin-Assisted Biodegradable Polymer Assemblies for Electrostatic-Driven Drug Delivery. *Chem. - Asian J.* **2014**, *9*, 1365−1372.
(38) Moses, M. A.; Brem, H.; Langer, R. Advancing the Field of Drug Delivery: Taking Aim at Cancer. *Cancer Cell* **2003**, *4*, 337−341.
(39) Casals, E.; Puntes, V. F. Inorganic Nanoparticle Biomolecular Corona: Formation, Evolution and Biological Impact. *Nanomedicine (London, U. K.)* **2012**, *7*, 1917−1930.
(40) Moore, T.; Chen, H.; Morrison, R.; Wang, F.; Anker, J. N.; Alexis, F. Nanotechnologies for Noninvasive Measurement of Drug Release. *Mol. Pharmaceutics* **2014**, *11*, 24−39.
(41) Shahbazi, M.-A.; Almeida, P.; Mäkilä, E. M.; Kaasalainen, M. H.; Salonen, J. J.; Hirvonen, J. T.; Santos, H. A. Augmented Cellular Trafficking and Endosomal Escape of Porous Silicon Nanoparticles via Zwitterionic Bilayer Polymer Surface Engineering. *Biomaterials* **2014**, *35*, 7488−7500.

DOI: 10.1021/acsami.5b07033
ACS Appl. Mater. Interfaces 2015, 7, 23197−23204